American Journal of Applied Mathematics
2025; 13(4): 274-281
http://www.sciencepublishinggroup.com/j/ajam
doi: 10.11648/j.ajam.20251304.14
ISSN: 2330-0043 (Print); ISSN: 2330-006X (Online)

Modified Spectral Quasilinearization Method for Solving Fluid Flow over Stretching Sheet

Mwatela James Mwakio[1, *], Samuel Mutua[1], Felicien Habiyaremye[2]

[1]Department of Mathematcs, Statistics and Physical Sciences, Taita Taveta University, Voi, Kenya
[2]Department of Mathematics and Actuarial Sciences, The Catholic University of Eastern Africa, Nairobi, Kenya

Email address:
mwakiojames@gmail.com (Mwatela James Mwakio), mutua.samuel@ttu.ac.ke (Samuel Mutua),
fhabiyaremye@cuea.edu (Felicien Habiyaremye)
[*]Corresponding author

To cite this article:
Mwatela James Mwakio, Samuel Mutua, Felicien Habiyaremye. (2025). Modified Spectral Quasilinearization Method for Solving Fluid Flow over Stretching Sheet. *American Journal of Applied Mathematics, 13*(4), 274-281. https://doi.org/10.11648/j.ajam.20251304.14

Received: 11 June 2025; **Accepted:** 30 June 2025; **Published:** 5 August 2025

Abstract: This study aims to develop an efficient and accurate numerical method for solving the boundary layer fluid flow over a stretching sheet using a modified spectral quasilinearization method. The governing partial differential equations (PDEs) for momentum and energy are first transformed into a system of nonlinear ordinary differential equations (ODEs) using similarity transformations. The improvement in the method of solution is realized by numerically solving the flow equations defined over a larger semi-infinite domain $[0, \infty)$ using spectral quasilinearization method embedded on overlapping sub-intervals. This method is better than its counterpart on a single domain as it maintains high accuracy and at the same time results in a sparse differentiation matrix that is easily invertible and saves CPU time. The numerical simulations and solution error analysis were performed using MATLAB version 2018a. Convergence analysis demonstrates exponential error decay, with residual errors reducing from the order of 10^{-2} to approximately 10^{-12} within four iterations, confirming the accuracy and efficiency of the numerical scheme. Additionally, the impact of the Prandtl number on thermal boundary layer thickness is examined, revealing sharper temperature gradients for higher Pr values. This method can be adapted to solve other fluid flow problems represented as systems of nonlinear ODEs.

Keywords: Stretching Sheet, Spectral Quasilinearization Method, Overlapping Sub-intervals, Similarity Transformation

1. Introduction

This section introduces the physical and mathematical background of boundary layer flow over a stretching sheet, with emphasis on the importance of such flows in engineering and industrial applications. A review of relevant studies is provided, covering effects of magnetic fields, nonlinear radiation and variable fluid properties. The Spectral Quasilinearization Method (SQLM), a numerical technique combining spectral collocation and quasilinearization, is presented as a suitable tool for solving such flow problems efficiently. The motivation for this study is discussed, and the governing partial differential equations are shown to be transformed into linear ordinary differential equations, which are then solved numerically over a semi-infinite domain using overlapping grids.

The quasi-linearization method was successfully used to solve coupled system of ODEs by Muraza, Shateyi and Marewo [1] In their study, the numerical results were verified by comparison with the exact solution. Analysis of boundary layer flow of an incompressible fluid over a stretching sheet has gained attention due to its applications in engineering and industrial processes e.g., cooling of electronic devices and nuclear reactors. Researchers have so far investigated various aspects of this flow ranging from flow past linearly stretching plate [2] in 2-D and many others who all discussed some characteristics towards a stretching sheet in presence of magnetic field, slip effect, convective boundary conditions etc. considering different types of fluids like nanofluids, viscoelastic, and micropolar fluids. The study of magnetic field effects has important applications in engineering and science. The interaction of magnetic field with nanofluids can be utilized in overcoming cooling challenges nuclear reactors and inductive the flow meters, which rely on the potential difference in the fluid in the direction perpendicular to the motion and to the magnetic field. The importance of non-Newtonian nanofluids has attracted attention of many researchers due to their various applications in mechanical, chemical and engineering processes. Casson fluid model is one of the non-Newtonian fluid models which gives yield stress. If shear stress is less than yield stress, then the fluid behaves like a solid, and if shear stress is greater than yield stress, the fluid starts moving. Examples of Casson fluids include honey, jelly, tomato sauce, blood and concentrated fruit juice. Casson fluid model has possible applications in polymer industries and biomechanics. Owing to these applications, many authors have studied the characteristics of Casson fluid along stretched surface. Mukhopadhyay and Vajravelu [3] analyzed MHD flow and heat transfer of Casson fluid over a stretching surface. They considered MHD flow, heat and mass transfer of Casson fluid over an unsteady stretching surface. Butt et al. [4] explored unsteady three-dimensional flow of Casson fluid over a stretching surface. Radiative heat transfer on viscous flow occurs when there exist temperature differences between the surrounding and the ambient fluid. Radiation effects play an important role in controlling heat transfer processes in polymer industry. In most studies, radiation is taken as constants in the flow region. However, it is difficult to maintain the constant temperature in the entire flow region, thus incorporating nonlinear radiation become necessary.

Nonlinear thermal radiation plays a significant role in many industrial, scientific and technological applications. As shown by Afify [5], Hall effects emerge in ionized fluid when the conductivity normal to the magnetic field diminishes because of the spiralling of electrons and ions about the magnetic lines of the force before the collisions and a current is induced in a direction normal to both the electric and magnetic fields. Studies on MHD flow, heat and mass transfer where Hall current is considered can be utilized in various industrial and engineering applications. Pal [6] scrutinized the effects of Hall current and thermal radiation on MHD flow and heat transfer of a viscous fluid over an unsteady stretched surface. Ashraf et al. [7] studied MHD mixed convection flow of a Casson fluid along a stretching surface with Hall Effect. El-Aziz et al. [8] examined Hall effects on MHD slip flow of Casson nanofluid along a stretching sheet. Prashu and Nandkeolyar [9] used spectral quasi-linearization method to analyze three-dimensional flow of Casson fluid induced by a stretched surface with radiation and Hall effects. The efficiency of heat transfer in fluids is mostly dependent on their physical features. Among these features, viscosity and thermal conductivity are significant factors in the heat transfer process. Viscosity and thermal conductivity have been taken as constants in most studies conducted, for instance Matos and Oliveira [10]. However, fluid properties may vary significantly with temperature. To accurately analyze flow and heat transfer processes it is necessary to consider variable viscosity and thermal conductivity. Animasaun [11] investigated Casson fluid flow past an exponentially stretching sheet with variable viscosity and thermal conductivity. He also studied the effects of thermophoresis, variable viscosity and thermal conductivity on MHD Casson fluid flow along a vertical porous plate with suction. Bisht and Sharma [12] investigated flow of Casson nanofluid past a vertical nonlinear stretching surface with variable viscosity and thermal conductivity. Motivated by the studies and importance of obtaining accurate results while minimizing computational time, the objective of this study is to obtain an exact solution to a flow model over a stretching sheet using spectral quasi-linearization method. The governing partial differential equations of this flow are transformed into linear ordinary differential equations and solved numerically using spectral quasi-linearization method over a semi-infinite domain on overlapping grids.

2. Mathematical Formulation of the Problem

Consider steady flow of an incompressible newtonian fluid over a linearly stretching sheet. The fluid is at a steady-state flow, and the velocity of stretching is given by $u_w = ax$ where a is the constant stretching rate at $y = 0$ and x is the distance from the edge. The fluid occupies the region $y > 0$ and due to this motion a boundary layer develops along the surface with the fluid exhibiting velocity components $u(x, y)$ in the horizontal direction and $v(x, y)$ in the vertical direction. Figure 1 also shows the boundary layer thickness $\delta(x)$ which increases with distance from the edge.

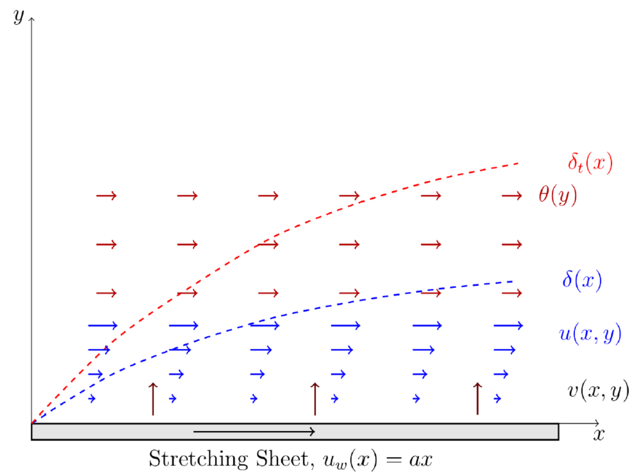

Figure 1. *Sketch of the Physical Problem.*

2.1. Flow Equations

Assuming a steady incompressible two-dimensional Newtonian flow, with no slip, low temperature gradients over a linearly stretching sheet, the governing equations for this study are;

The continuity equation is given by:

$$\frac{\partial u}{\partial x}+\frac{\partial v}{\partial y}=0 \tag{1}$$

The momentum equation is given by:

$$u\frac{\partial u}{\partial x}+v\frac{\partial u}{\partial y}=\nu\frac{\partial^2 u}{\partial y^2} \tag{2}$$

where; $\nu=\frac{\mu}{\rho}$ is the kinetic viscosity of the fluid
μ is the dynamic viscosity of the fluid
ρ is the density of the fluid given by:
$\rho=\rho_f$
The energy equation is given by:

$$u\frac{\partial T}{\partial x}+v\frac{\partial T}{\partial y}=\alpha\frac{\partial^2 T}{\partial y^2} \tag{3}$$

Where,

1. u, v: velocity components in the x- and y-directions
2. T: temperature
3. $\alpha=\dfrac{k}{\rho c_p}$: thermal diffusivity
4. x: streamwise coordinate
5. y: coordinate normal to the sheet

Boundary conditions

For a linearly stretching sheet, the boundary conditions are given by:

$$\begin{aligned}&\text{At } y=0: \quad u=U_w(x)=ax, \quad v=0, \quad T=T_w,\\ &\text{As } y\to\infty: \quad u\to 0, \quad T\to T_\infty,\end{aligned} \tag{4}$$

To convert the governing equations into a set of nonlinear ordinary differential equations we introduce the following similarity transformations;

$$u=\frac{\partial\psi}{\partial y} \quad v=-\frac{\partial\psi}{\partial x} \quad \theta(\eta)=\frac{T-T_\infty}{T_w-T_\infty}, \quad \eta=\sqrt{\frac{a}{\nu}}y \tag{5}$$

where the similarity variable η is defined as:

1. a: represents a characteristic parameter related to the stretching velocity.
2. ν: is the kinematic viscosity of the fluid.
3. y: denotes the vertical distance from the surface.

with the stream function ψ defined as;
$\psi=\sqrt{a\nu}xf(\eta)$
With the help of equation 5, the governing equations, 2, 3 becomes;

$$f'''(\eta)+f(\eta)f''(\eta)-f'^2(\eta)=0 \tag{6}$$

$$\theta''+Prf(\eta)\theta'=0 \tag{7}$$

And the corresponding boundary conditions, 4 becomes;

$$\begin{aligned}&\text{At } y=0: \quad f(0)=0, \quad f'(0)=1, \quad \theta(0)=1\\ &\text{As } y\to\infty: \quad f'(\infty)=0, \quad \theta(\infty)=0,\end{aligned} \tag{8}$$

3. Numerical Method of Solution

The set of coupled non-linear governing boundary layer equations (2) and (3) together with boundary conditions (4) are solved numerically by using Spectral Quasilinearisation Method. First of all, the higher order non-linear differential equations (2) and (3) are converted into simultaneous linear ordinary differential equations using quasilinearisation method.

Applying the Quasilinearization Method (QLM) [15] to the momentum equation (6), we obtain the linearized residual form:

$$R_1=\alpha_{3r}f_r'''+\alpha_{2r}f_r''+\alpha_{1r}f_r'+\alpha_{0r}f_r-L_1[f_r''',f_r'',f_r',f_r]$$

where the coefficients are given by:

$$\alpha_{3r}=-1, \quad \alpha_{2r}=-f_r, \quad \alpha_{1r}=2f_r', \quad \alpha_{0r}=-f_r''$$

Substituting and simplifying:

$$R_1=-f_r'''-f_rf_r''+2f_r'f_r'-f_r''f_r-\left(f_r'^2-f_rf_r''-f_r'''\right)$$

yields the simplified form:

$$R_1=f_r'^2-f_rf_r'' \tag{9}$$

Similarly, applying QLM to the energy equation (7), we obtain:

$$R_2=\gamma_{0r}f_r+\beta_{2r}\theta_r''+\beta_{1r}\theta_r'-L[\theta_r''+\mathrm{Pr}f_r\theta_r']$$

with coefficients:

$$\gamma_{0r}=\mathrm{Pr}\,\theta_r', \quad \beta_{2r}=1, \quad \beta_{1r}=\mathrm{Pr}f_r$$

Substituting and simplifying:

$$R_2=\mathrm{Pr}\,\theta_r'f_r+\theta_r''+\mathrm{Pr}f_r\theta_r'-\theta_r'-\mathrm{Pr}f_r\theta_r'$$

results in:

$$R_2=\mathrm{Pr}f_r\theta_r' \tag{10}$$

The semi infinite domain $[0,\infty)$ is truncated into a finite domain $[0,L]$ where L is taken to be large enough to approximate conditions at infinity.

The computational domain $[0,L]$ is decomposed into a set of M overlapping sub intervals of equal lengths.

For application in MATLAB, the computational domain $[0,L]$ is set as $[0,100]$ and decomposed to 10 overlapping subintervals (M) and 10 collocation points (N).

Each subinterval $E_k, k=1,2,...M$ is discretized into $N+1$ Chebyshev Gauss Lobato points defined by;

$$z_i=cos(\frac{\pi i}{N}), \qquad i=0,1,2,...,N, \qquad z\epsilon[-1,1]$$

The points $z_i, i=0,1,2,...,N$ are mapped into respective subintervals using the linear transformation;

$$\eta_i = \frac{\overset{R}{E_k} - \overset{L}{E_k}}{2} z_i + \frac{\overset{L}{E_k} + \overset{R}{E_k}}{2}$$

where $\overset{L}{E_k}$ and $\overset{R}{E_k}$ represent the left and right end of the k^{th} subinterval.

The solution $f(\eta)$ at the k^{th} subinterval is approximated by the Lagrange interpolating polynomial;

$$F(\eta) = \sum_{j=0}^{N} L_j(\eta) F_j$$

Where $L_j(\eta)$ is the Lagrange cardinal polynomial defined by:

$$L_j(\eta) = \prod_{\substack{k=0 \\ k\neq j}}^{N} \frac{\eta - \eta_k}{\eta_j - \eta_k}, \quad L_j(\eta_i) = \begin{cases} 1, & \text{if } i = j, \\ 0, & \text{if } i \neq j. \end{cases}$$

The First order derivative in each sub-interval is approximated by;

$$F'(\eta) = \sum_{j=0}^{N} L'_j(\eta) F_j$$

At the collocation points the first order derivative is approximated by

$$F'(\eta_i) = \sum_{j=0}^{N} L'_j(\eta_i) F_j$$

$$F'(\eta_i) = \sum_{j=0}^{N} D_{ij} F_j \tag{11}$$

Where D is the Chebyshev Differential Matrix as defined in [16]

In vector form, equation 11 is written as;

$$F' = DF$$

where $F = [f(\eta_0), f(\eta_1), f(\eta_2), ..., f(\eta_N)]^T$

The differential matrix over the entire computational domain is assembled as;

$$\mathbf{D} = \begin{bmatrix} D_{1,0} & D_{1,1} & \dots & D_{1,N-1} & D_{1,N} & & & \\ D_{2,0} & D_{2,1} & \dots & D_{2,N-1} & D_{2,N} & & & \\ \ddots & \ddots & & \ddots & \ddots & & & \\ D_{N-1,0} & D_{N-1,1} & \dots & D_{N-1,N-1} & D_{N-1,N} & & & \\ & & & D_{1,0} & D_{1,1} & \dots & D_{1,N_{x-1}} & D_{1,N} \\ & & & D_{2,0} & D_{2,1} & \dots & D_{2,N_{x-1}} & D_{2,N} \\ & & & \ddots & \ddots & & \ddots & \ddots \\ & & & D_{N-1,0} & D_{N-1,1} & \dots & D_{N-1,N-1} & D_{N-1,N} \end{bmatrix}$$

The empty entries in the matrix above are all zeros.

Higher order derivatives are approximated using matrix multiplication;

$$F'' = D^2 F, \qquad F''' = D^3 F$$

Derivatives for unknown θ are approximated in a similar manner.

Using the approximate discrete derivatives, the QLM Scheme 9 and 10 becomes;

$$[\alpha_{3r} D^3 + \alpha_{2r} D^2 + \alpha_{1r} D + \alpha_{0r}] F = R_1 \tag{12}$$

$$\gamma_{0r} F + [\beta_{2r} D^2 + \beta_{1r} D]\theta = R_2 \tag{13}$$

Equations 12 and 13 can be written as;

$$\begin{bmatrix} A_{11} & A_{12} \\ A_{21} & A_{22} \end{bmatrix} \begin{bmatrix} F \\ \theta \end{bmatrix} = \begin{bmatrix} R_1 \\ R_2 \end{bmatrix} \tag{14}$$

Where;

$$\begin{aligned} A_{11} &= \alpha_{3r} D^3 + \alpha_{2r} D^2 + \alpha_{1r} D + \alpha_{0r} I \\ A_{12} &= 0 \\ A_{21} &= \gamma_{0r} I \\ A_{22} &= \beta_{2r} D^2 + \beta_{1r} D \end{aligned}$$

The boundary conditions 8 are evaluated at collocation points as;

$$f(\eta_N) = 0, \qquad \sum_{j=0}^{N} D_{Nj}F_j = 1, \qquad \sum_{j=0}^{N} D_{0j}F_j = 0, \qquad \theta(\eta_N) = 1, \qquad \theta(\eta_0) = 0 \tag{15}$$

Boundary conditions 15 are imposed onto a matrix system as;

$$\left[\begin{array}{cccc|cccc} D_{00} & D_{01} & \dots & D_{0N} & 0 & 0 & \dots & 0 \\ \hline & & A_{11} & & & & A_{12} & \\ \hline D_{N0} & D_{N1} & \dots & D_{NN} & 0 & 0 & \dots & 0 \\ 0 & 0 & \dots & 1 & 0 & 0 & \dots & 0 \\ \hline 0 & 0 & \dots & 0 & 1 & 0 & \dots & 0 \\ \hline & & A_{21} & & & & A_{22} & \\ \hline 0 & 0 & \dots & 0 & 0 & \dots & 0 & 1 \end{array}\right] \left[\begin{array}{c} F_0 \\ \hline \vdots \\ \hline F_{N-1} \\ F_N \\ \hline \theta_0 \\ \hline \vdots \\ \hline \theta_N \end{array}\right] = \left[\begin{array}{c} 0 \\ \hline R_1 \\ \hline 1 \\ 0 \\ \hline 0 \\ \hline R_2 \\ \hline 1 \end{array}\right] \tag{16}$$

The initial approximation to solution to start the iteration process are chosen to be arbitrary exponential functions that satisfy the boundary questions and are given by;
$f(\eta) = 1 - e^{-\eta} \qquad \theta(\eta) = e^{-\eta}$
These initial functions are not only simple and smooth but also satisfy the boundary conditions exactly and exhibit the expected boundary layer decay behavior. $f(0) = 0$, $f'(0) = 1$, $\theta(0) = 1$, and both $f'(\eta)$ and $\theta(\eta)$ decay to zero as $\eta \to \infty$. This choice is also supported by their successful use in similar fluid flow studies e.g. [2] and [14] because of their compatibility with spectral methods.

4. Results and Discussion

Computation for the Prandtl number Pr is done. For illustration of the results, the numerical values are plotted in figures for the dimensionless temperature profile and are consistent with the results obtained by [13] and [14].

Table 1. *Comparison of $q(0) = -\theta'(0)$ for various Prandtl numbers using SQLM, HAM [14], and FEM [2].*

Pr	Present (SQLM)	HAM [14]	FEM [2]
0.72	7.1172×10^{-4}	7.12×10^{-4}	7.11×10^{-4}
1.00	7.1917×10^{-5}	7.18×10^{-5}	7.20×10^{-5}

To assess the accuracy of the method, residual error analysis is conducted, and respective results for momentum and energy equations are plotted. From the graphs, it is evident that the method is highly accurate, as the residual errors are on the order of 10^{-8} for the momentum equation and 10^{-12} for the energy equation.

To assess the convergence of the numerical method, solution error analysis is performed, and the numerical values are plotted against the number of iterations.

The solution errors for f and θ were measured using the infinity norm ($\|\cdot\|_\infty$), defined as the maximum absolute difference between successive iterations at all collocation points.

$$\|e_f\|_\infty = \max_i |f_i^{(k)} - f_i^{(k-1)}|,$$

$$\|e_\theta\|_\infty = \max_i |\theta_i^{(k)} - \theta_i^{(k-1)}|,$$

where $f_i^{(k)}$ and $\theta_i^{(k)}$ denote the values of f and θ at the i-th collocation point during iteration k.

The method shows a rapid convergence within the first four iterations.

Table 2. *Residual errors for function F and temperature profile θ over 10 iterations.*

Iteration	Residual of F	Residual of θ
1	3.5172×10^{-5}	3.4566×10^{-4}
2	2.8986×10^{-8}	1.9111×10^{-8}
3	1.2835×10^{-8}	2.2258×10^{-12}
4	1.9209×10^{-8}	3.1966×10^{-12}
5	5.2096×10^{-9}	3.6380×10^{-12}
6	1.0956×10^{-8}	2.3211×10^{-12}
7	2.9020×10^{-8}	4.2411×10^{-12}
8	1.6591×10^{-8}	3.6380×10^{-12}
9	3.8448×10^{-8}	5.5280×10^{-12}
10	1.2054×10^{-8}	2.8294×10^{-12}

Table 3. *Solution errors for function F and temperature profile θ over 10 iterations.*

Iteration	Solution error of F	Solution error of θ
1	1.91484×10^{-2}	1.97412×10^{-1}
2	6.94991×10^{-5}	6.28701×10^{-4}
3	2.69531×10^{-9}	1.27896×10^{-8}
4	9.70557×10^{-12}	1.21791×10^{-12}
5	7.04836×10^{-12}	5.83089×10^{-13}
6	4.61187×10^{-12}	6.47316×10^{-13}
7	5.28166×10^{-12}	1.52311×10^{-12}
8	3.65408×10^{-12}	1.01524×10^{-12}
9	1.13608×10^{-11}	1.12438×10^{-12}
10	2.24343×10^{-11}	2.32842×10^{-12}

The numerical results demonstrate that the modified spectral quasilinearization method exhibits high accuracy and rapid convergence when applied to the boundary layer fluid flow over a stretching sheet. The residual error analysis shows that the momentum equation achieves residuals on the order of 10^{-8}, while the energy equation reaches residuals as low as 10^{-12}, indicating a high level of numerical precision. Additionally, the solution error decreases sharply within the first four iterations, confirming the method's fast convergence. This convergence behavior and residual performance validate the robustness and effectiveness of the proposed method in solving nonlinear boundary layer problems with high computational efficiency.

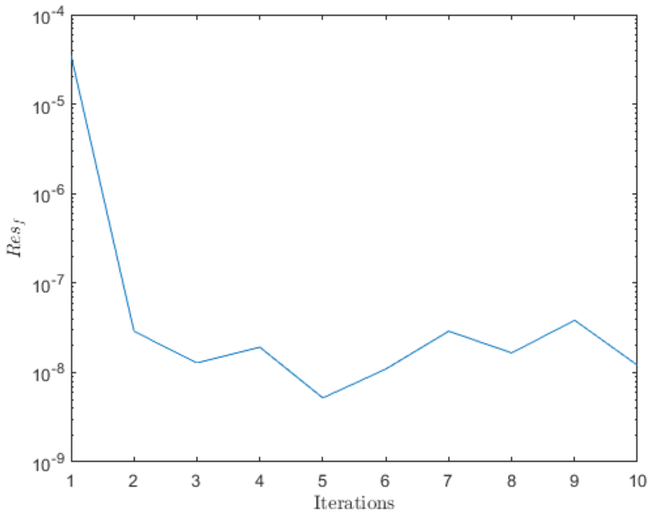

(a) Residuals for momentum equation.

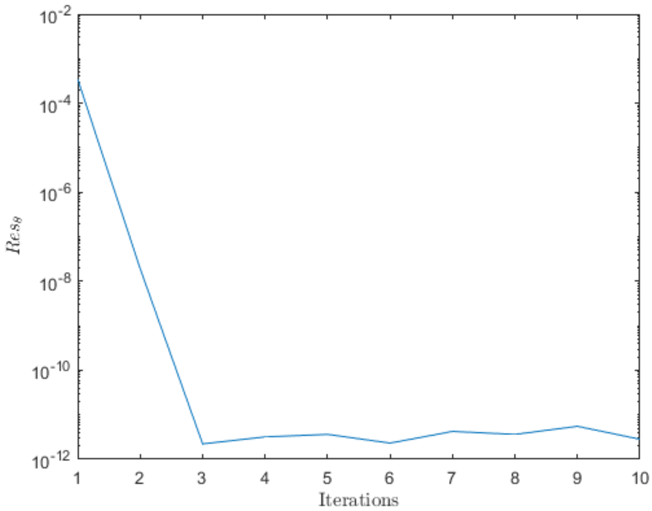

(b) Residuals for energy equation.

Figure 2. *Residual error plots for accuracy check.*

Figure 2 shows that a rapid exponential decay is achieved within the first 3 iterations where the residuals fall below 10^{-8} for momentum equation and 10^{-11} for energy equation, exhibiting a high numerical accuracy. The convergence behavior of the momentum residual Res_f shows a rapid drop in the initial iterations then the residual exhibits slight oscillations rather than a strictly monotonic decrease. This non-monotone convergence is characteristic of spectral quasilinearization approaches, attributed to the global interpolation properties of Chebyshev polynomials and the nonlinear nature of the problem. Nevertheless, the residual consistently remains below the convergence threshold, verifying the accuracy of the method.

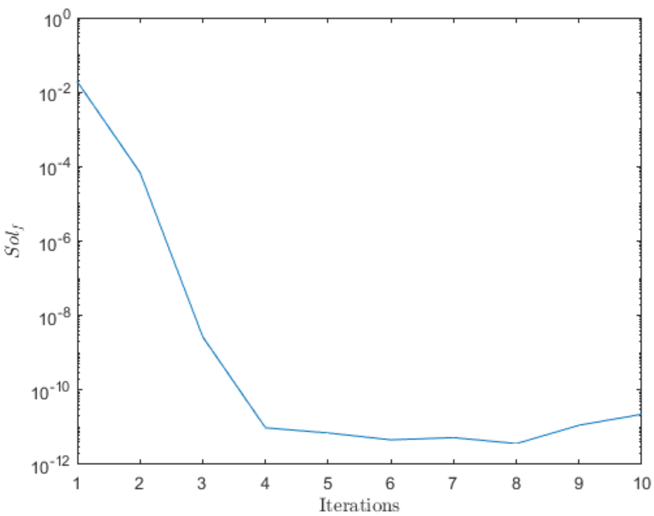

(a) Solution error for momentum equation.

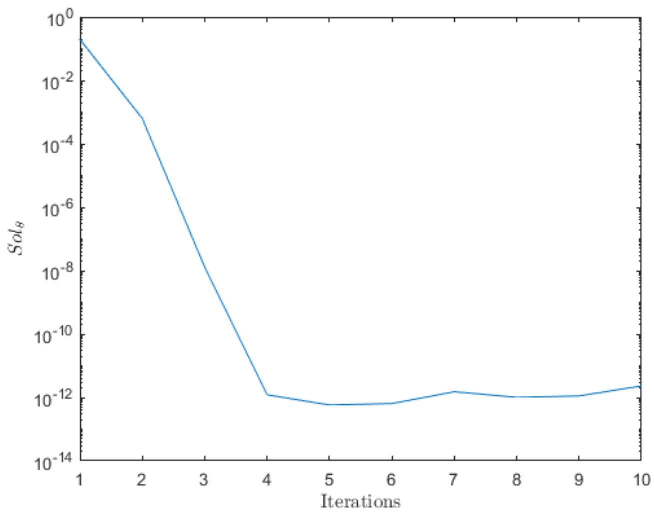

(b) Solution error for energy equation.

Figure 3. *Convergence check using solution error plots.*

Figure 3 shows solution error profiles for momentum and energy across 10 iterations of the proposed SQLM. Both solution errors show a rapid exponential decay stabilizing at approximately 10^{-12} after just four iterations. This behavior confirms quadratic convergence characteristic of the QLM-based framework with the momentum equation converging slightly faster initially while the energy equation demonstrating consistent convergence throughout.

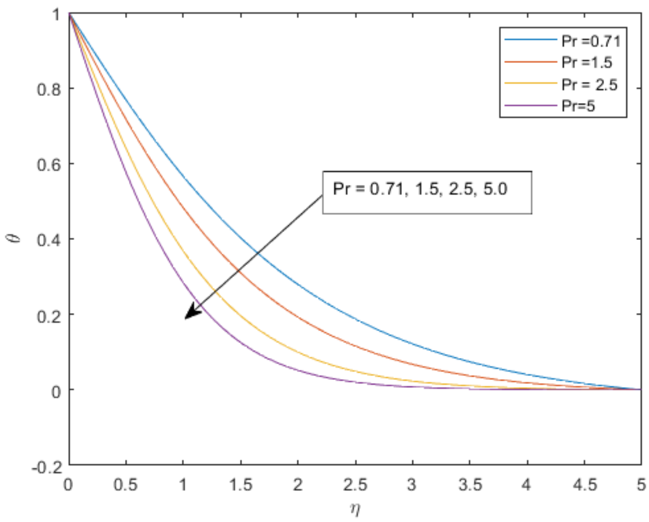

Figure 4. *Temperature Profiles for Various Prandtl Numbers.*

Figure 4 illustrates the temperature distribution $\theta(\eta)$ across the boundary layer for various Prandtl numbers Pr $= 0.72, 1.00, 1.50, 2.50$. As the Prandtl number increases, the thermal boundary layer becomes progressively thinner, indicating enhanced thermal confinement. This trend aligns with physical expectations: higher Prandtl numbers correspond to fluids with lower thermal diffusivity, which results in steeper temperature gradients near the surface and a more rapid decay of temperature away from the wall. The results demonstrate the capability and accuracy of the proposed SQLM method in resolving temperature profiles across a broad range of Prandtl numbers.

To support this observation, Table 4 provides the computed wall heat flux values $q(0) = -\theta'(0)$ for each Prandtl number. The decreasing trend in wall heat flux with increasing Pr confirms the accuracy of the temperature profiles. These results validate the ability of the proposed SQLM approach to resolve boundary layer characteristics effectively across a wide range of Prandtl numbers.

Table 4. *Computed wall heat flux $q(0) = -\theta'(0)$ for various Prandtl numbers.*

Prandtl Number (Pr)	$\mathbf{q(0) = -\theta'(0)}$
0.72	7.1172×10^{-4}
1.00	7.1917×10^{-5}
1.50	1.0443×10^{-6}
2.50	1.7731×10^{-10}

5. Conclusions

This study presents a numerical solution of boundary layer fluid flow over a stretching sheet. The SQLM embedded on overlapping subintervals is used to solve the governing equations. The overlapping grid technique reduces the size of the differential matrix making it easy to invert. Quasilinearization is essential in simplifying the complex non-linear PDEs to ODEs which are simpler to analyze and solve. The main findings of this study can be summarised as follows:

1. As the Prandtl number increases, a boundary layer constriction is observed. This is followed by a more rapid decline in temperature as the similarity variable η increases. This is due to decrease in thermal diffusivity which prevents thermal energy diffusion away from the stretching surface.
2. The results obtained using the modified Spectral Quasilinearization Method (SQLM) with overlapping subintervals demonstrate the effectiveness of this approach in solving the fluid boundary layer flow problem over a stretching sheet. The numerical findings confirm the high accuracy and rapid convergence of the method, as seen from the residual and solution error analyses. Residual errors in the momentum and energy equations reach orders as low as 10^{-8} and 10^{-12} respectively, validating the numerical accuracy of the SQLM.
3. The overlapping subintervals ensure smooth convergence and high spatial accuracy. This makes the SQLM a reliable and efficient method for studying complex fluid boundary layer phenomena. The method's ability to accurately resolve steep gradients and nonlinearities confirms its applications in broader fluid dynamic studies, particularly in scenarios requiring high-resolution numerical techniques. Overall, the findings reinforce SQLM as a robust and effective computational approach for analyzing nanofluid boundary layers.

The specific objectives set out at the beginning of this study have been successfully achieved:

1. The governing equations for fluid flow over a stretching sheet were formulated using boundary layer theory.
2. Similarity transformations were applied to reduce the nonlinear partial differential equations into a system of ordinary differential equations, suitable for numerical treatment.
3. A modified Spectral Quasilinearization Method incorporating overlapping subintervals was developed and effectively applied to solve the resulting system of equations with high accuracy and rapid convergence.

The modified SQLM with overlapping subintervals from the results proves to be highly accurate, computationally efficient and stable method for solving fluid flows over stretching surfaces, offering a promising tool for future studies involving boundary layer flows and other challenging nonlinear PDE systems.

ORCID

0009-0003-1994-321X (Mwatela James Mwakio)
0009-0007-4363-6729 (Felicien Habiyaremye)

Acknowledgments

The author thanks Dr. Samuel Mutua and Dr. Felicien Habiyaremye for their valuable guidance throughout this research and Taita Taveta University for providing me with the opportunity to undertake my research, and my family and friends for their constant support and motivation.

Author Contributions

Mwatela James Mwakio: Conceptualization, Methodology, Validation, Writing - original draft
Samuel Mutua: Software, Supervision, Writing - review & editing
Felicien Habiyaremye: Supervision, Validation

Conflict of Interest

The authors declare that there is no conflict of interest regarding the publication of this paper.

References

[1] H. Muzara, S. Shateyi, and G. Marewo, "Spectral quasi-linearization method for solving the Bratu problem," *Advances and Applications in Fluid Mechanics*, vol. 21, pp. 449–463, 2018. https://doi.org/10.17654/FM021040449

[2] Crane, L. J., "Flow past a stretching plate," *Zeitschrift fÃ¼r Angewandte Mathematik und Physik*, vol. 21, pp. 645–647, 1970.

[3] S. Mukhopadhyay, "Casson fluid flow and heat transfer over a nonlinearly stretching surface," *Chinese Physics B*, vol. 22, 074701, 2013.

[4] Butt, A. S., Tufail, M. N., and Ali, A., "Three-dimensional flow of a magnetohydrodynamic Casson fluid over an unsteady stretching sheet embedded into a porous medium," *Journal of Applied Mechanics and Technical Physics*, vol. 57, pp. 283–292, 2016.

[5] A. A. Afify, "MHD free convective flow and mass transfer over a stretching sheet with chemical reaction," *Heat and Mass Transfer*, vol. 40, no. 6, pp. 495–500, 2004.

[6] D. Pal, "Hall current and MHD effects on heat transfer over an unsteady stretching permeable surface with thermal radiation," *Computers & Mathematics with Applications*, vol. 66, no. 7, pp. 1161–1180, 2013.

[7] Ashraf, M. B., Hayat, T., and Alsaedi, A., "Mixed convection flow of Casson fluid over a stretching sheet with convective boundary conditions and Hall effect," *Boundary Value Problems*, vol. 2017, pp. 1–17, 2017.

[8] M. A. El-Aziz and A. A. Afify, "Effect of Hall current on MHD slip flow of Casson nanofluid over a stretching sheet with zero nanoparticle mass flux," *Thermophysics and Aeromechanics*, vol. 26, pp. 429–443, 2019.

[9] Prashu and R. Nandkeolyar, "A numerical treatment of unsteady three-dimensional hydromagnetic flow of a Casson fluid with Hall and radiation effects," *Results in Physics*, vol. 11, p. 966, 2018.

[10] H. M. Matos and P. J. Oliveira, "Steady flows of constant-viscosity viscoelastic fluids in a planar T-junction," *Journal of Non-Newtonian Fluid Mechanics*, vol. 213, pp. 15–26, 2014.

[11] Animasaun, I. L., Adebile, E. A., and Fagbade, A. I., "Casson fluid flow with variable thermo-physical property along exponentially stretching sheet with suction and exponentially decaying internal heat generation using the homotopy analysis method," *Journal of the Nigerian Mathematical Society*, vol. 35, no. 1, pp. 1–17, 2016.

[12] A. Bisht and R. Sharma, "Non-similar solution of Casson nanofluid with variable viscosity and variable thermal conductivity," *International Journal of Numerical Methods for Heat & Fluid Flow*, ahead-of-print, 2019.

[13] R. Cortell, "Viscous flow and heat transfer over a nonlinearly stretching sheet," *Applied Mathematics and Computation*, vol. 184, no. 2, pp. 864–873, 2007. https://doi.org/10.1016/j.amc.2006.06.077

[14] S. J. Liao, *Beyond Perturbation: Introduction to the Homotopy Analysis Method*. CRC Press, 2003.

[15] Bellman, R., Kalaba, R. E., and Leondes, C. T., *Quasilinearization and Nonlinear Boundary-value Problems*. American Elsevier Publishing Company, 1965.

[16] L. N. Trefethen, "IV.21 Numerical Analysis," in *The Princeton Companion to Mathematics*, T. Gowers, J. Barrow-Green, and I. Leader, Eds., illustrated ed. Princeton, NJ, USA: Princeton University Press, 2008.